Journal of NeuroVirology
https://doi.org/10.1007/s13365-024-01216-9

Suppression of HIV-TAT and cocaine-induced neurotoxicity and inflammation by cell penetrable itaconate esters

B. Celia Cui[1] · Marina Aksenova[1] · Aliaksandra Sikirzhytskaya[1] · Diana Odhiambo[1] · Elizaveta Korunova[1] · Vitali Sikirzhytski[1] · Hao Ji[1] · Diego Altomare[1] · Eugenia Broude[1] · Norma Frizzell[2] · Rosemarie Booze[3] · Michael D. Wyatt[1] · Michael Shtutman[1]

Received: 17 November 2023 / Revised: 20 April 2024 / Accepted: 20 May 2024
© The Author(s) 2024

Abstract

HIV-associated neurological disorder (HAND) is a serious complication of HIV infection marked by neurotoxicity induced by viral proteins like Tat. Substance abuse exacerbates neurocognitive impairment in people living with HIV. There is an urgent need for therapeutic strategies to combat HAND comorbid with Cocaine Use Disorder (CUD). Our analysis of HIV and cocaine-induced transcriptomes in primary cortical cultures revealed significant overexpression of the macrophage-specific gene aconitate decarboxylase 1 (Acod1). The ACOD1 protein converts the tricarboxylic acid intermediate cis-aconitate into itaconate during the activation of inflammation. Itaconate then facilitates cytokine production and activates anti-inflammatory transcription factors, shielding macrophages from infection-induced cell death. However, the immunometabolic function of itaconate was unexplored in HIV and cocaine-exposed microglia. We assessed the potential of 4-octyl-itaconate (4OI), a cell-penetrable ester form of itaconate known for its anti-inflammatory properties. When primary cortical cultures exposed to Tat and cocaine were treated with 4OI, microglial cell number increased and the morphological altercations induced by Tat and cocaine were reversed. Microglial cells also appeared more ramified, resembling the quiescent microglia. 4OI treatment inhibited secretion of the proinflammatory cytokines IL-1α, IL-1β, IL-6, and MIP1-α induced by Tat and cocaine. Transcriptome profiling determined that Nrf2 target genes were significantly activated in Tat and 4OI treated cultures relative to Tat alone. Further, genes associated with cytoskeleton dynamics in inflammatory microglia were downregulated by 4OI treatment. Together, the results strongly suggest 4-octyl-itaconate holds promise as a potential candidate for therapeutic development to treat HAND coupled with CUD comorbidities.

Keywords HAND · Microglia · Itaconate · Acod 1 · Neuroinflammation · HIV · Tat

Abbreviations

ART	Antiretroviral therapy
PLWH	People living with HIV
HAND	HIV-associated neurocognitive disorder
CUD	Cocaine use disorder
BBB	Blood brain barrier
CNS	Central nervous system
IRG1	Immune responsive gene 1
Acod1	Aconitate decarboxylase 1
4OI	4-Octyl-itaconate
Nqo1	NAD(P)H quinone oxidoreductase 1
Gstp1	Glutathione S-transferase Pi
Gclc	Glutamate cysteine ligase catalytic subunit
VASP	Vasodilator Stimulated Phosphoprotein

B. Celia Cui and Marina Aksenova contributed equally.

✉ Michael Shtutman
shtutmanm@cop.sc.edu

[1] Department of Drug Discovery and Biomedical Sciences, College of Pharmacy, University of South Carolina, Columbia, SC 29208, USA

[2] Department of Pharmacology, Physiology and Neuroscience, School of Medicine, University of South Carolina, Columbia, SC 29208, USA

[3] Department of Psychology, College of Arts and Sciences, University of South Carolina, Columbia, SC 29208, USA

Introduction

Human immunodeficiency virus type 1 (HIV-1) affects over 38 million individuals globally and over 1.2 million people in the United States (NIDA). The rise of antiretroviral

Published online: 17 June 2024

therapy (ART) has effectively suppressed viral replication in people living with HIV (PLWH) and made the life expectancy of PLWH comparable to that of individuals without HIV infection. Nonetheless, PLWH continue to bear a disproportionately heavier burden of major comorbidities, experiencing these health challenges more than 16 years prior to the general population (Marcus et al. 2020).

One of the most debilitating complications of HIV infection results in neurocognitive dysfunction referred to as HIV-associated neurological disorder (HAND). Despite the advent of ART, nearly 50% of PLWH continue to suffer from HAND. This condition encompasses a spectrum of neurological dysfunctions, spanning asymptomatic neurocognitive impairment and mild neurocognitive disorder, to HIV-associated dementia, which results in severe cognitive deficits and memory loss (Saylor et al. 2016). Given the considerable burden on affected individuals' quality of life, it is crucial to alleviate the neurotoxicity of HIV infection in the cells of the central nervous system (CNS). Microglial cells, despite being only 15% of total brain cells, play a vital role in HIV infection within the CNS. They serve as the primary site for viral infection and replication, as well as the main reservoir and source of viral latency in the brain. Moreover, microglia contribute significantly to HIV reactivation and the development of a chronic cerebral inflammatory state (Sreeram et al. 2022; Wallet et al. 2019).

Reportedly, all HIV proteins, including transactivator of transcription (Tat), gp120, gag, env, have been shown to exert neurotoxic effects on the progression of CNS pathology (Nath 2002; Yuan et al. 2015). Among these proteins, Tat is considered one of the most toxic, and functions as an early regulatory protein essential for the replication capacity of the virus. Tat mediates HIV gene expression and controls the complex pattern of protein expression necessary for functional viral transcription (Karn and Stoltzfus 2012). Additionally, Tat is highly implicated in intracellular pathways that lead to significant pro-inflammatory cytokine overproduction in macrophages (Ben Haij et al. 2015; Zayyad and Spudich 2015).

Compounding the HIV-associated neuropathology, there is a strong correlation between substance use disorders and the exacerbation of HAND (Beyrer et al. 2010; Gannon et al. 2011). Notably, cocaine, one of the most abused drugs in the US (NIDA 2018), is frequently used among PLWH. The concomitant use of HIV and cocaine has been shown to significantly contribute to HIV pathogenesis. Adding to this, HIV-infected patients with cocaine use disorder (CUD) often experience worsened HAND (Atluri 2016; Avants et al. 1997). Previous studies have revealed that cocaine can activate immune responses and induce the expression of pro-inflammatory cytokines from BV2 microglia cells (Liao et al. 2016). While the combined consequences of Tat and cocaine are multifaceted, our specific focus centers on understanding how the interactions between Tat and cocaine contribute to the induction of neuroinflammation through microglia (Zhao et al. 2022).

Current ART drugs struggle to adequately penetrate blood brain barrier (BBB), are prone to effective removal from brain parenchyma, and as a result, fail to combat HIV reservoir formation and persistence in the brain (Osborne et al. 2020). Regrettably, there is currently no approved therapy available for the treatment of HAND, especially for the neurological consequences resulting from concurrent HIV infection and drug abuse. However, targeting aberrant microglial activity has emerged as a potential therapeutic approach for treating both neurogenerative diseases and drug addiction (Biber et al. 2019; Catale et al. 2019; Liu et al. 2019). As a result, microglia infected with the virus and the resulting inflammatory response triggered by the toxic HIV proteins are increasingly recognized as a disease-associated microglial state that requires further investigation. Previously, we have uncovered that the inhibition of microglial activation via a small molecule inhibitor can protect neurons from the combined Tat and cocaine toxicity, suggesting that microglia can be a valuable target in HAND-CUD treatment (Aksenova et al. 2019).

We observed an increased expression of aconitate decarboxylase 1 (Acod1) based on RNA sequencing analysis of Tat-and cocaine-treated primary cortical cultures. Acod1, also known as immune responsive gene 1 (IRG1), catalyzes the synthesis of itaconate by decarboxylating the tricarboxylic acid cycle intermediate cis-aconitate, which shunts this carbon skeleton out of the TCA cycle (Michelucci et al. 2013). Itaconate can be added to protein thiols through a process called dicarboxypropylation and alter their activity or function. Notably, itaconate is emerging as an essential regulator of immune metabolism, displaying high levels in activated macrophages and influencing in their metabolic functions and inflammatory responses (O'Neill and Artyomov 2019). Considering that HIV-induced metabolic dysfunction is exacerbated by cocaine (Samikkannu et al. 2016), itaconate becomes even more intriguing in the context of this virus.

Recent studies have investigated the immunomodulatory properties of 4-octyl-itaconate (4OI), a membrane and BBB penetrable ester-modified itaconate. In particular, 4OI has demonstrated potent anti-inflammatory effects and has been shown to significantly reduce inflammatory responses to a variety of pathogenic viruses such as SARS-CoV-2, Herpes Simplex Virus-1 and -2, Zika and Vaccinia (Olagnier et al. 2020b; Sohail et al. 2022b). The anti-inflammatory effect of itaconate is mediated in part by its ability to regulate immune function and inflammation by delaying pyroptotic cell death (Bambouskova et al. 2021), attenuating the excessive production of reactive oxygen species (Sohail et al. 2022b), promoting anti-inflammatory transcription factor Nuclear respiratory factor (2Nrf2) through Nrf2-Keap1 signaling

pathway (Mills et al. 2018; Ni et al. 2022), and inhibiting pro-inflammatory cytokine production (Lampropoulou et al. 2016).

However, the role of the Acod1/itaconate axis in HIV-1 and cocaine-induced neurotoxicity is unknown. To investigate, we tested the effects of the cell-permeable itaconate derivative 4OI in Tat and cocaine-treated primary rat fetal cortical cultures. Our study reveals, for the first time, that 4OI can provide neuroprotection against Tat and cocaine neurotoxicity in vitro. Additionally, we observed 4OI-induced changes in microglia and conducted transcriptomic analyses on these cell cultures to obtain a better understanding of the underlying mechanisms.

Materials and methods

Neuronal cell cultures

Primary rat fetal mixed neuronal cultures were prepared from 18-day-old Sprague–Dawley rat fetuses (Envigo Laboratories, Indianapolis, IN) as described previously (Aksenova et al. 2019, 2009) in accordance with the University of South Carolina Institutional Animal Care and Use Committee. Briefly, tissue was dissected, incubated in a solution of 0.05% Trypsin/EDTA, washed with Hank's balanced salt solution (HBSS, Thermo Fisher Scientific), dissociated by trituration and distributed into poly-L-lysine coated 12-well plates (Costar, Cambridge, MA) with and without inserted glass coverslips containing DMEM/F12 medium with 10% fetal bovine serum. After 24 h initial plating medium was replaced with serum-free Neurobasal medium supplemented with 2% B-27, 2 mM GlutaMAX and 0.5% D-glucose. All reagents were from Thermo Fisher Scientific. Half of the medium was replaced with freshly prepared medium once a week. Cultured cells were used for experiments at the age of 3 weeks in vitro (DIV 21).

Experimental treatment

Primary rat cortical cultures were treated with recombinant Tat 1–86 (Diatheva, Italy) and with cocaine-HCl (Sigma Chemicals) as described in each Figure Legend. The concentrations of Tat and cocaine were selected in accordance with our previous experimental data (Aksenova et al. 2019), and stock solutions were prepared as previously described. 4OI was obtained from Cayman Chemicals (Catalog No. 25374, Ann Arbor, MI). A stock solution of itaconate was prepared as a 50 mM stock in DMSO and was diluted to final concentrations from 30 µM up to 250 µM.

The concentration of Tat used in our study was chosen to reflect those found in the sera of HIV-positive patients (Xiao et al. 2000) and in cerebrospinal fluid (Westendorp et al. 1995). Similarly, the concentrations of cocaine used in the study were chosen based on animal studies that involved drug self-administration, which were suggested to parallel those found in recreational human users (Zimmer et al. 2011) and postmortem brain tissues in fatal cases of cocaine abuse (Spiehler and Reed 1985).

Apoptotic/dead cells detection

Dead and apoptotic cells were detected using the CellEvent Caspase-3/7 Kit (#C10423, Thermo Fisher Scientific) according to the manufacturer's recommendations. Briefly, after experimental treatment, Caspase3/7 Green Detection Reagent was added directly to cells, and the plate was incubated for 30 min at 37 °C. During the final 5 min of incubation, SYTOX AADvanced dead cell solution was added. Cells were rinsed with PBS, and images of cells were taken immediately. Alternatively, cells were fixed with 4% paraformaldehyde, imaged, and used for further experiments.

Immunocytochemistry

For ICC analysis cells were plated on glass coverslips and placed inside 12-well plates. Following experimental treatment, primary cortical cultures were fixed with 4% paraformaldehyde (EM Sciences, Hatfield, PA) and permeabilized with 0.1% Triton X-100. Fixed cultures were blocked with 10% fetal bovine serum for 2 h and then co-labeled overnight with the following primary antibodies: chicken polyclonal anti-MAP2 antibodies (1:2,000) (# ab92434, Abcam, Cambridge MA) or rabbit monoclonal anti-Iba1 (1:300) (# ab178847 Abcam, Cambridge MA). Secondary antibodies, goat anti-chicken IgG conjugated with AlexaFluor 594, and goat anti-rabbit IgG conjugated with AlexaFluor 488 (1:500 both; Invitrogen Life Technologies, Grand Island NY), were used for visualization. To identify cell nuclei, DAPI was added with the final PBS wash, and coverslips were mounted on glass slides using ProLong Glass Antifade Mount (Invitrogen Life Technologies, Eugene, OR).

Image processing and analysis

Images were captured on a Carl Zeiss LSM 700 laser scanning confocal microscope (Carl Zeiss Meditec, Dublin, CA) equipped with 20x (Plan APO 0.8 air) objective. Images were captured using 0.7 scanning zoom with 312-nm X–Y pixel size. Fluorescence and differential interference contrast (DIC) imaging was done using single-frame mode.

ImageJ software (National Institutes of Health, USA) was used for manual analysis of microscopy images acquired using a Zeiss 700 confocal microscope. Several fields of vision were taken from at least three different wells. The total number of cells and percentage of Iba1 positive cells were estimated using segmentation of DNA channel (DAPI) followed by

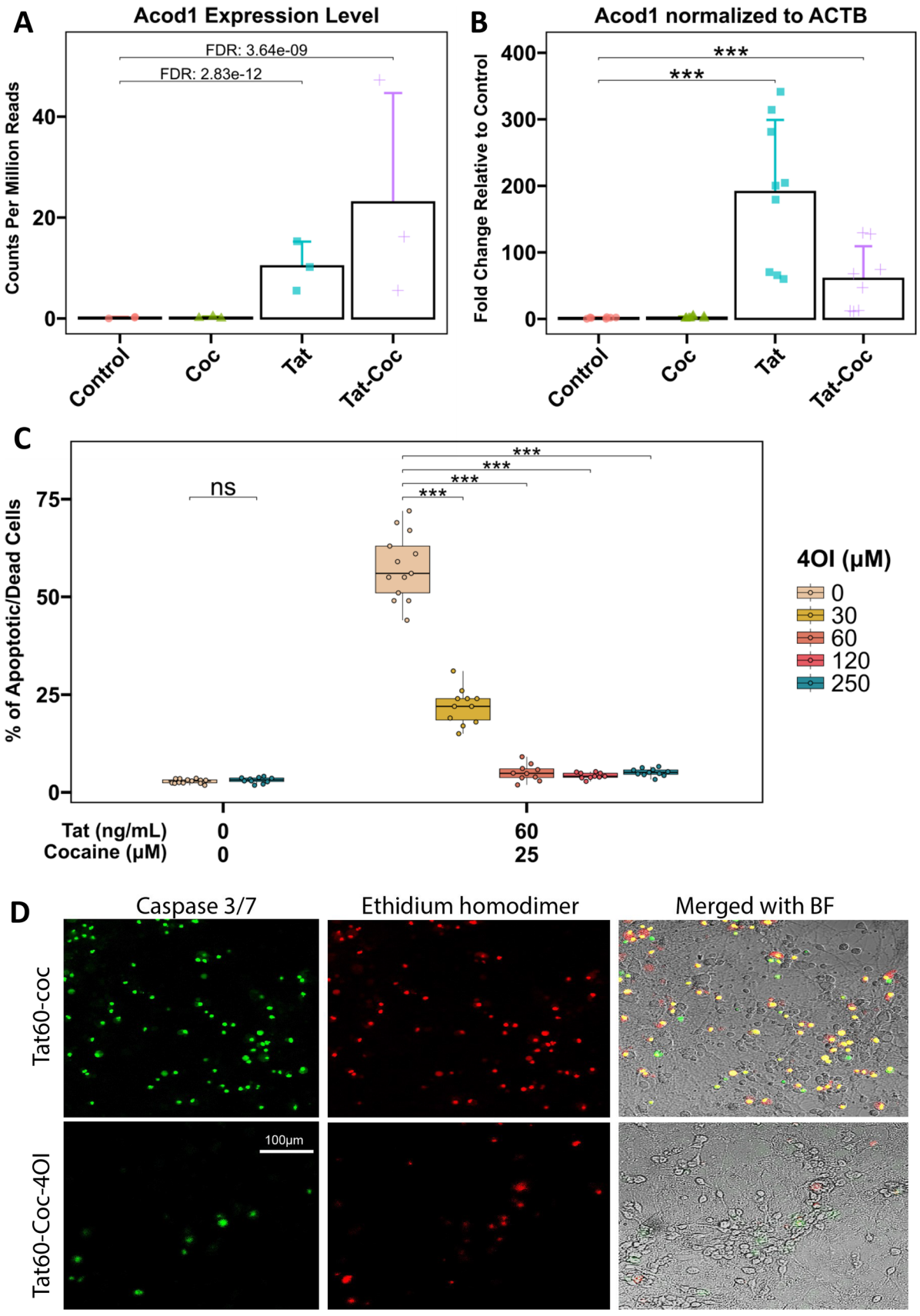
A
Acod1 Expression Level
FDR: 3.64e-09
FDR: 2.83e-12
Counts Per Million Reads
0
20
40
Control
Coc
Tat
Tat-Coc
B
Acod1 normalized to ACTB
***
***
Fold Change Relative to Control
0
100
200
300
400
Control
Coc
Tat
Tat-Coc
C
% of Apoptotic/Dead Cells
0
25
50
75
ns
***
***
***
***
Tat (ng/mL)
Cocaine (μM)
0
0
60
25
4OI (μM)
0
30
60
120
250
D
Caspase 3/7
Ethidium homodimer
Merged with BF
Tat60-coc
Tat60-Coc-4OI
100μm

◂**Fig. 1** Acod1 expression in Tat and/or cocaine-treated primary neuronal cultures, and neuroprotective effects of 4OI. **a** Acod1 expression was assessed in primary cortical cultures treated with cocaine (25 µM) alone for 24 h, Tat (6 ng/mL) alone for 48 h, or Tat for 48 h followed by the addition of cocaine for 24 h. Acod1 levels were quantified using RNA-seq and presented as CPM read counts. **b** qPCR analysis of the same experimental samples measured Acod1 expression fold change, normalized to ACTB. Statistical analysis was performed using the Mann–Whitney/Wilcoxon Rank-Sum test, followed by Bonferroni's post hoc test. **c** Boxplots illustrate the dose-dependent effect of 4OI (30, 60, 120, or 250 µM) on Tat (60 ng/mL) and cocaine (25 µM) treated cultures. Non-treated control cultures and cultures treated with the highest concentration of 4OI (250 µM) are shown on the left. Each data point represents an image containing 300–450 cells. Statistical significance was determined using the Mann–Whitney-Wilcoxon test, followed by Bonferroni post hoc test (ns: not significant; *: $p<0.05$; **: $p<0.01$; ***: $p<0.001$). **d** Immunofluorescent staining of cultures treated with Tat (60 ng/mL) with or without 4OI (250 µM) for 48 h followed by cocaine (25 µM) for 24 h, fixed with 4% PFA. Dead/apoptotic cells were detected using the CellEvent Caspase 3/7 Assay Kit (Green: Caspase 3/7; Red: Ethidium Bromide). Scale bar: 100 µm

"Analyze Particles" ImageJ command. Size of microglial cells and length of microglia processes were estimated individually using "Freehand selections" and "Freehand lines" ImageJ tool. Data were aggregated, analyzed and visualized using R ggplot2 tools. Background correction of widefield images was performed using the background (Gaussian blur) division procedure (32-bit mode), followed by an image histogram adjustment for a 16-bit dynamic range.

Cytokine/chemokine array

Medium was collected from each culture well at the end of each experiment, frozen, and sent to Eve Technologies Corporation (Calgary, Canada) for LUMINEX-based analysis of cytokines by Featured-Rat Cytokine Array/ Chemokine Array 27-plex (RD27). The 27-plex array analyzed Eotaxin, EGF, Fractalkine, IFN-γ,IL-1α, IL-1β, IL-2, IL-4, IL-5, IL-6, IL-10, IL-12 (p70), IL-13, IL-17A, IL-18, IP-10, GRO/KC, TNF-αalpha, G-CSF, GM-CSF, MCP-1, Leptin, LIX, MIP-1αalpha, MIP-2, RANTES, VEGF. The level of cytokines in each sample had been measured thrice to provide technical triplicates.

RNA sequencing

RNA and library preparation, post-processing of the raw data and data analysis were performed by the USC CTT COBRE Functional Genomics Core. RNAs were extracted using Zymo Quick-RNA MicroPrep Kits as per manufacturer recommendations (Zymo Research, Irvine, CA, USA). RNA quality was evaluated on RNA-1000 chips using a Bioanalyzer (Agilent, Santa Clara, CA, USA). RNA libraries were prepared using an established protocol with NEBNExt Ultra II Directional Library Prep Kit (NEB, Lynn, MA). Each library was made with one of the TruSeq barcode index sequences and the Illumina sequencing done by Medgenome (Foster City, CA) with Illumina NovaSeq PE100 (100 bp, pair-ended). Sequences were aligned to the Rat genome Rnor_6.0 (GCA_000001895.4, ensemble release-99) using STAR v 2.7.2b (Dobin et al. 2013). Samtools (v1.2) was used to convert aligned sam files to bam files and reads were counted using the featureCounts function of the Subreads package (Liao et al. 2014) and the Rattus_norvegicus.Rnor_6.0.93.gtf annotation file. Only reads that were mapped uniquely to the genome were used for gene expression analysis. Differential expression analysis was performed in R using the edgeR package (Robinson et al. 2010). Raw counts were normalized using the Trimmed Mean of M-values (TMM) method and the normalized read counts were then fitted to a generalized linear model using the function glmFit (McCarthy et al. 2012). Genewise tests for significant differential expression were performed using the function glmLRT. The P-value was then corrected for multiple testing using Benjamini-Hochburg's FDR.

Data analysis and statistics

Graphs were generated using Inkscape version 1.3. Data visualization and analysis were performed using R v4.3.1 with ggplot2 v3.4.3 in RStudio v2023.06.1 + 524 using custom code. The Mann–Whitney-Wilcoxon Test followed by Bonferroni correction were utilized for statistical comparisons of relevant experimental groups, unless specified otherwise. All data are represented as mean ± SD unless otherwise stated, with $p<0.05$ regarded as statistically significant.

Results

Transcriptomic profiles of Tat and cocaine treated primary cortical cultures reveals differential expression of Acod1

To investigate the impact of Tat and cocaine on the transcriptome of primary cortical cultures, we previously performed RNA sequencing analysis on cultures treated with Tat alone, cocaine alone, or a combination of both (Aksenova et al. 2019). Analysis of the transcriptome upregulated by Tat or Tat-Cocaine treatment revealed a significant increase in the expression of Acod1 (Fig. 1A). To corroborate this finding, we performed qPCR analysis measuring the expression of Acod1 normalized to the reference control beta-actin (ACTB) expression within the same experimental cultures. The qPCR results confirmed a significant increase in Acod1 expression relative to the control for Tat only or Tat and cocaine treatment groups (Fig. 1B).

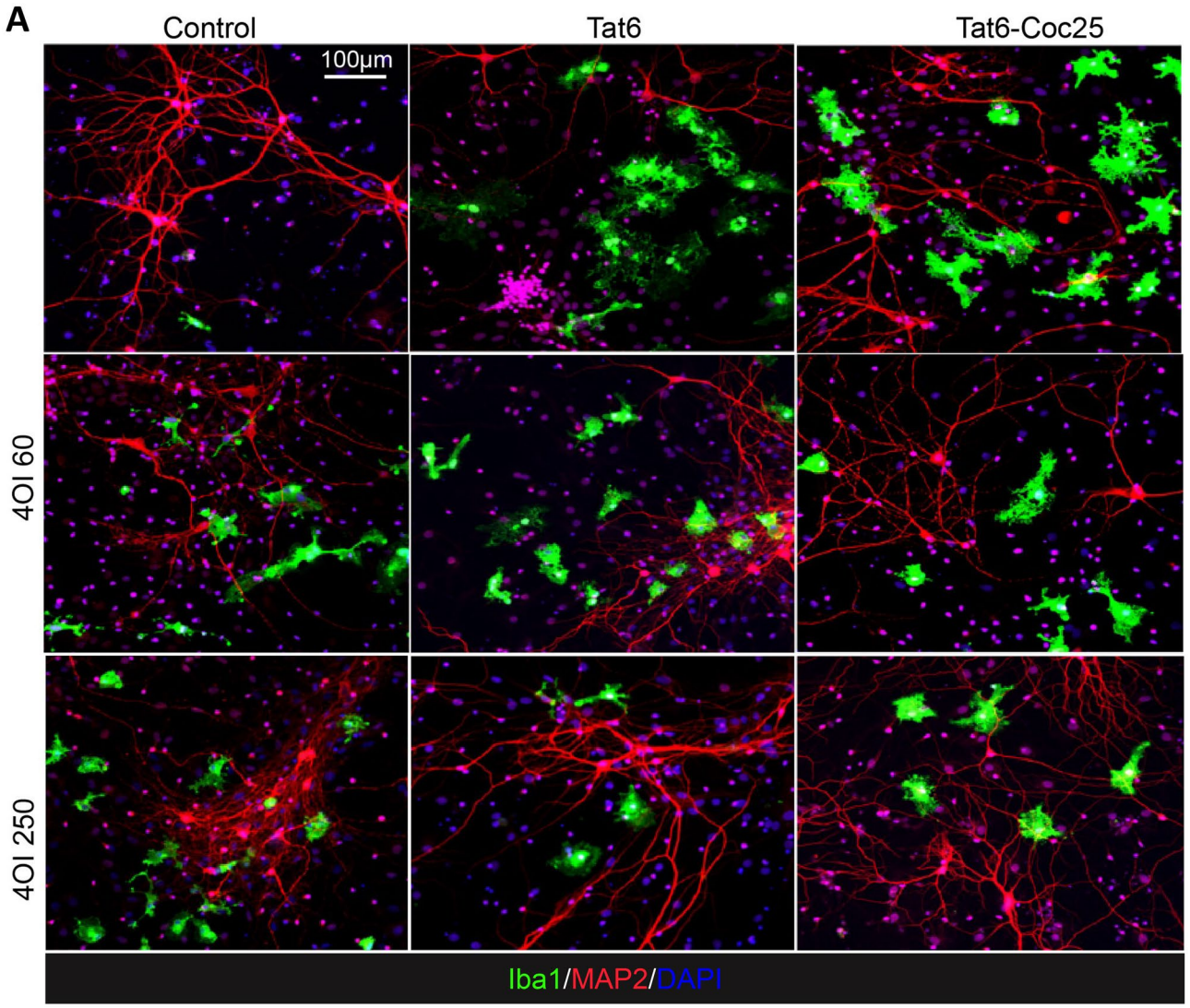
A
Control
Tat6
Tat6-Coc25
100μm
4OI 60
4OI 250
Iba1/MAP2/DAPI

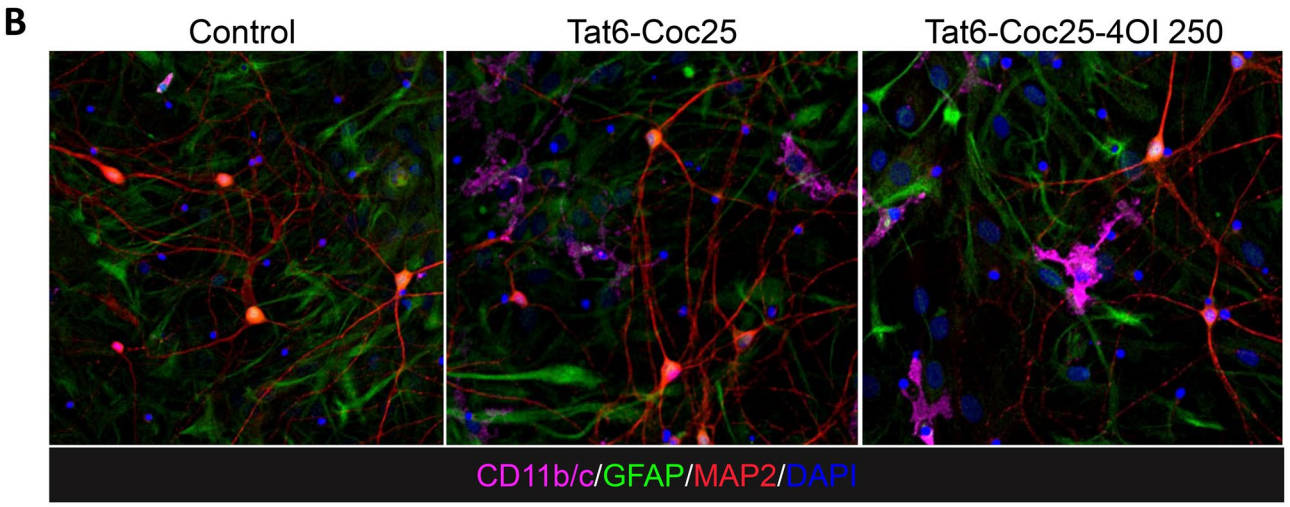
B
Control
Tat6-Coc25
Tat6-Coc25-4OI 250
CD11b/c/GFAP/MAP2/DAPI

◂**Fig. 2** Effects of 4OI treatment on microglia morphology in Tat and/or cocaine-treated primary neuronal cultures. Immunofluorescent staining of primary cortical cultures: **a** Cells were treated with Tat alone (6 ng/ml) or Tat combined with 4OI (60 or 250 µM) for 48 h, followed by cocaine (25 µM) for additional 24 h. Cells were fixed with 4% PFA. Staining: Iba1 (green, microglia marker), MAP2 (red, neuronal marker), DAPI (blue, nuclei). Scale bar: 100 µm. **b** Cells were subjected to the same treatment. Staining: CD11b/c (magenta, activated microglia marker), GFAP (green, astrocyte marker), MAP2 (red, neuronal marker), DAPI (blue, nuclei)

Although the role of Acod1 in the context of HAND has not been examined, there is a rapidly emerging recognition of the importance of its product, the metabolite itaconate, in cellular inflammatory pathways and in the progression of various viral infections (Olagnier et al. 2020a; Sohail et al. 2022a). In particular, the introduction of exogenous itaconate was shown to exhibit antiviral effects and to curtail inflammatory responses (Daniels et al. 2019). Thus, we chose to evaluate the effects of itaconate in this HAND-CUD model.

Neuroprotective effect of 4-octyl-itaconate against Tat and cocaine combined neurotoxicity in primary cortical cultures.

After identifying Acod1 as a Tat and Tat-Cocaine upregulated gene, (Fig. 1A-B), we evaluated the effects of itaconate, the product of cis-aconitate decarboxylation by Acod1. Because itaconate in its cytosolic form is not cell-permeable, we opted to use its membrane-penetrable ester-modified derivative, 4-octyl itaconate (4OI), to investigate the effects of metabolic modulation on microglia function in our HAND and CUD primary culture model that uses the Tat protein and cocaine as the neurotoxic insults. Consistent with our previous study, treatment of the cortical cultures with Tat (1, 6, or 60 ng/mL) or cocaine (10 or 25 µM) individually at the doses tested did not result in significant cell death, while the combination of Tat and cocaine resulted in concentration-dependent neuronal death (Supplemental Fig. 1A). The combined neurotoxic effect was not observed when cortical cultures were treated with heat-inactivated Tat combined with cocaine. The regimen of Tat and cocaine treatment was selected as previously performed to model transient cocaine exposure of PLWH, and concentrations correspond to the concentration of Tat and cocaine in the brains of HIV-infected patients and in cocaine self-administrating rodents. (Aksenov et al. 2006; Aksenova et al. 2019, 2009).

The administration of 4OI successfully reversed the detrimental effects of the combined Tat and cocaine toxicity (Fig. 1C-D, Fig. 2), with a decrease in cell death due to 4OI exhibiting a dose-dependent response (Fig. 1C). Based on these results, we identified 4OI doses of 60 µM and 250 µM as the lowest and highest concentrations that significantly rescued neuronal cell death under these conditions. These findings strongly suggested that treatment with 4OI can effectively rescue neurons from death caused by the presence of Tat and cocaine.

4OI modulates the morphological changes of microglia brought by Tat and cocaine treatment

The neuroinflammation induced by Tat or Tat-Cocaine treatment appeared to manifest in morphological changes observed in microglia. While treatment with cocaine alone did not affect microglia morphology (data not shown), the exposure to Tat alone or Tat-Cocaine resulted in an increased percentage of microglial cells (Supplemental Fig. 1B), accompanied by a greater occurrence of microglia exhibiting amoeboid-shape characteristics (Supplemental Fig. 1C-D). This ameboid shape is indicated by a reduction in process length and an increase in the cell body size of microglia. This effect was Tat and Tat-Cocaine concentration-dependent, except for the highest doses used in combination, which resulted in a decrease in the number of microglia cells and their body size commensurate with the increase in cell death at this highest combination dose (Supplemental Fig. 1).

Treating naïve cultures with 4OI alone also resulted in an increase in microglial cells displaying more ameboid characteristics (Fig. 3B-C). In particular, when cultures were treated with 250 µM 4OI (represented in dark blue), the median microglial processes shortened by about 5 µm, showing a 20% decrease, while the median size of microglial cell bodies expanded by about 250 μm^2, showing a 100% increase (Fig. 3B-C). Interestingly, microglia morphological profiles in cultures treated solely with 4OI closely resembled the activated microglia states observed in Tat-Cocaine treated cultures. This similarity was evident in the 3D spread of data representing total quantified microglia morphology representing percentages of cells by size and length. Specifically, the expanded spherical shape of the 3D plot showed a greater resemblance between the Tat-Cocaine and 4OI samples, in contrast to the control spread, which took a flat disk shape (Fig. 3D-E).

The effects of 4OI on microglia morphology were not unidirectional; instead, they were context dependent. The introduction of 4OI in Tat and cocaine treated cultures yielded opposing trends. For example, low Tat (6 ng/mL) and cocaine caused an increase in the percentage of Iba1-positive cells, along with a decrease in both microglia process length and cell body size, which were countered by 4OI treatment (Fig. 3A-C). Similarly, the effect of high Tat (60 ng/mL) and cocaine, which led to reduced Iba1-positive microglial cell percentage, microglia process length, and cell body size, were countered by 4OI administration (Supplemental Fig. 2A-C).

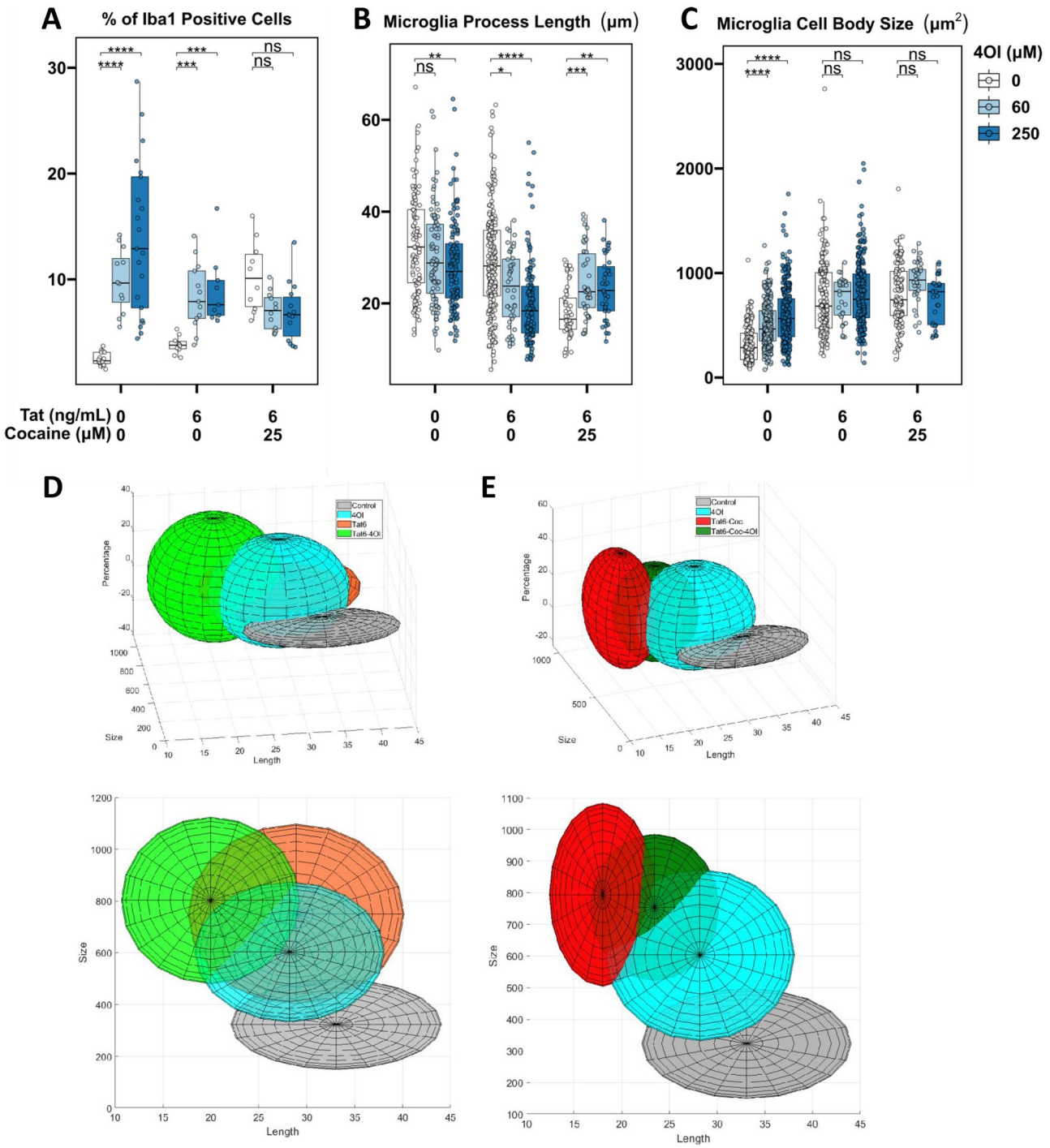

Fig. 3 Effects of Tat and cocaine on microglia cell morphology in primary neuronal cultures. **a** Proportion of Iba1 positive microglial cells in cultures treated with Tat (6 ng/mL) and/or 4OI (60 or 250 μM) for 48 h, with or without an additional 24 h of cocaine (25 μM). Tat-Coc vs Tat-Coc-4OI (60 μM) yielded not significant p-adj value = 0.126. Tat-Coc vs Tat-Coc-4OI (250 μM) yielded not significant p-adj value = 0.114. **b** Length of microglia processes and **c** microglia cell body size in the same cultures. The intensity of the blue color indicates increasing 4OI concentration (60, 250 μM). The box covers 50% of the data in each condition, and the line inside indicates the median value. The Mann–Whitney-Wilcoxon test was conducted to calculate the statistical significance, followed by Bonferroni post hoc test (ns, not significant; *, $p < 0.05$; **, $p < 0.01$; ***, $P < 0.001$). **d** 3D projection of microglia morphology affected by 4OI and/or Tat treatment. **e** 3D projection of microglia morphology affected by 4OI and/or Tat-Cocaine treatment (x: Body size; y: Percentage; z: Process length)

The 3D data spread illustrate that microglia treated with Tat-Cocaine-4OI were trending to the morphological state observed in 4OI-only treatments (Fig. 3D-E). Therefore, while 4OI mitigated Tat-Cocaine toxicity, 4OI alone also drove microglia towards an amoeboid morphological state.

RNA transcriptome of cell cultures treated with Tat, cocaine, and 4OI

To gain insights into the transcriptomic changes induced by Tat (6 ng/mL) or Tat and cocaine (25 µM) in primary cortical cultures with or without 4OI (250 µM) treatment, we conducted RNA-seq analysis (Supplemental Table 1). The bulk RNA sequencing findings were consistent with our earlier investigation (Aksenova et al. 2019), revealing a substantial impact of Tat treatment on the transcriptome (Fig. 4A). In contrast, the 24 h exposure to cocaine alone had a comparatively minimal effect on gene expression (Fig. 4C). In accordance with our previous results, the combined treatment Tat and cocaine yielded outcomes that closely mirrored those observed with Tat alone (Fig. 4B).

The pathway enrichment analysis of genes regulated by Tat alone or combined Tat-Cocaine exposure corroborated findings from other studies, demonstrating notable enrichment across diverse pathways. These included the adaptive immune response, complement binding, cytokine activity, and pathways regulated by NF-κB (Fig. 4A-B). Treatment with 4OI alone or in conjunction with Tat or Tat-Cocaine dramatically induced the expression of Nrf2 target genes (Fig. 4D-F, Supplementary Table 1-2). Remarkably, Nrf2 targeted pathways such as glutathione reduction antioxidant pathway involving NAD(P)H quinone oxidoreductase 1 (Nqo1), Glutathione S-transferase Pi (Gstp1), and glutamate cysteine ligase catalytic subunit (Gclc), displayed noteworthy activation exclusively in primary cortical cultures treated with 4OI (Fig. 4A-F). 4OI administration led to an upregulation of anti-inflammatory pathways, including Nrf2 target genes and antioxidant activity, alongside a downregulation of pro-inflammatory pathways such as cytokine activity and adaptive immune response (Fig. 4G-H). This enrichment of Nrf2 target gene pathways and antioxidant activities suggests a potential neuroprotective mechanism of 4OI in mitigating adverse neurotoxic effects.

Importantly, treatment with 4OI demonstrated a reduction in Tat-activated expression of well-known drivers of microglia inflammation, such as phosphodiesterase 4 (Pde4b) (Pearse and Hughes 2016) (Fig. 4I), along with P2 purinergic receptors P2rx4, P2ry2, and P2ry6 (Anwar et al. 2020; Hide et al. 2023; Sophocleous et al. 2022) (Fig. 4J). These purinergic receptors are recognized regulators of active phagocytosis and removal of stressed neurons (Puigdellivol et al. 2021). Moreover, the actin-binding proteins that coordinate phagocytosis, notably Vasodilator Stimulated Phosphoprotein (VASP) (Montaño-Rendón et al. 2022b), showed upregulation due to Tat-Cocaine treatment and downregulation in the presence of 4OI treatment (Fig. 4K). Similar trends were observed in the expression of pro-inflammatory cytokines, such as the interleukin and tumor necrosis factor families. Upregulation induced by Tat or Tat-Cocaine exposure was counteracted by 4OI administration, leading to downregulation (Fig. 4L-M, Supplemental Fig. 4).

Tat treatment led to a significant induction of Acod1 expression in comparison to the untreated control (Fig. 1A-B). This upregulated Acod1 expression induced by Tat or Tat-Cocaine was markedly diminished upon 4OI administration (Fig. 4E-F). Supported by additional qPCR analysis, the inclusion of 4OI exhibited a near three-fold reduction in Acod1 expression regardless of the presence of Tat or Tat-Cocaine, when compared to cultures treated with Tat alone (Supplemental Fig. 3A-B). Collectively, transcriptomic analysis of the experimental samples unveiled distinct gene expression patterns, providing insights into the specific influence of 4OI in modulating neuroinflammatory pathways.

4OI inhibition of pro-inflammatory cytokine secretion from Tat and cocaine treatment

We sought to uncover the functional consequences of 4OI administration on microglial cells in our primary mixed cultures, focusing on cytokine secretion as a key biomarker of inflammatory response. The release of pro-inflammatory cytokines serves as a widely recognized indicator of the detrimental effects associated with microglia activation (Hanisch 2002). To measure the levels of cytokines, we collected media from mixed cortical cultures treated with Tat followed by cocaine, with or without 4OI. We then determined the levels of 27 cytokines. The neuroinflammatory cytokines that had the greatest response to Tat-Cocaine are shown, with this treatment resulting in increased levels of IL-1α, IL-1β, IL-6, TNF-α, MIP-1α, MCP1, and LIX cytokines. 4OI treatment reduced the release of these cytokines by at least 30% (Fig. 5). In particular, the levels of IL-1α and IL-1β were reduced by > 50% in both the Tat-only or Tat-Cocaine treatment groups in the presence of 4OI. This data clearly shows that 4OI treatment suppresses the pro-inflammatory cytokine release profile of mixed cortical cultures.

Interestingly, the induction of IL-10 cytokine levels followed the exposure to Tat or Tat-Cocaine, which was notably suppressed with 4OI treatment. Although traditionally recognized as an anti-inflammatory cytokine, emerging evidence suggests that IL-10 can act as a modulator contributing to the formation and endurance of HIV reservoirs in non-primate HIV models (Harper et al. 2022). Our cell culture model aligns with and supports this evidence.

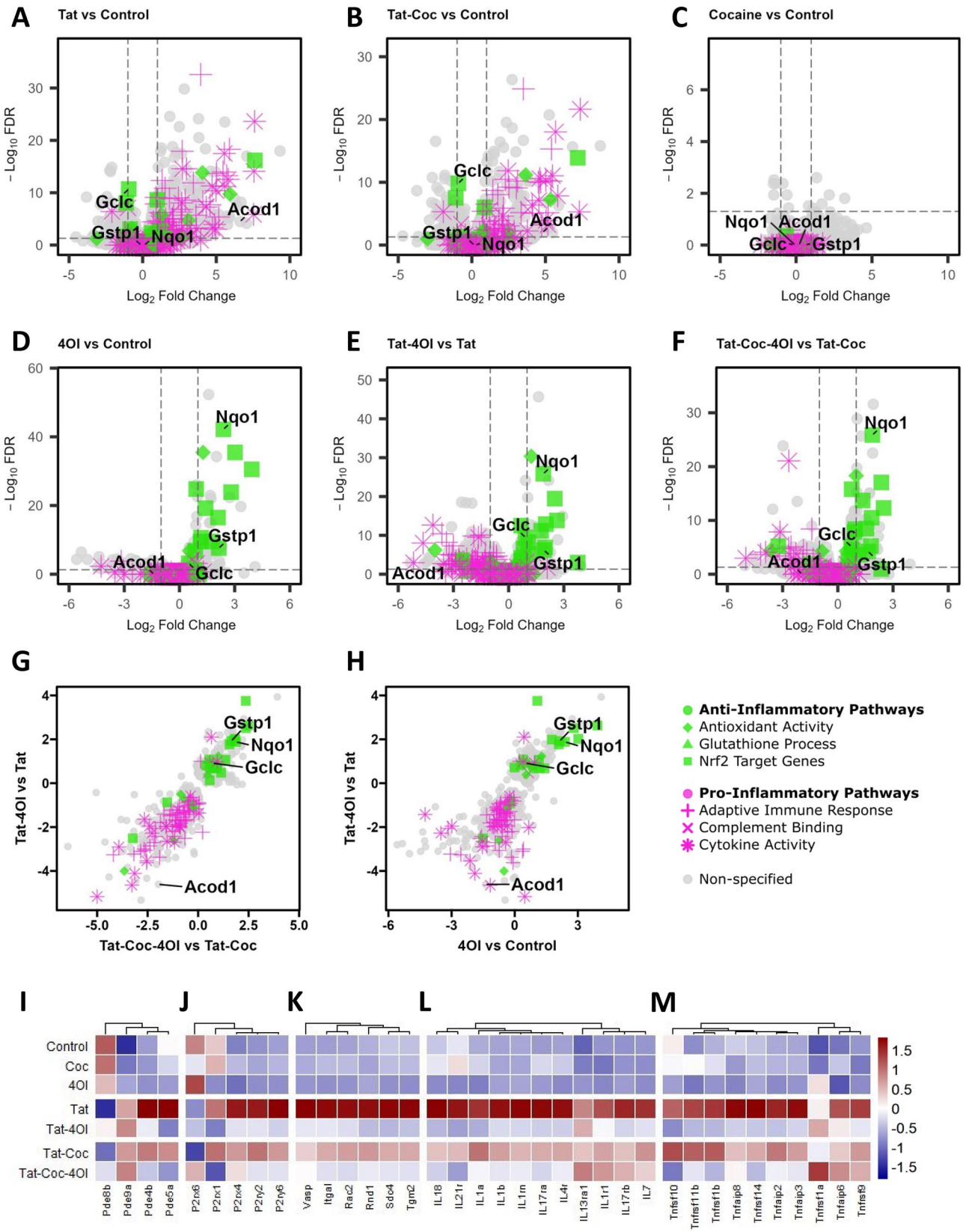
A
Tat vs Control
B
Tat-Coc vs Control
C
Cocaine vs Control
D
4OI vs Control
E
Tat-4OI vs Tat
F
Tat-Coc-4OI vs Tat-Coc
G
H
Gclc
Gstp1
Nqo1
Acod1
− Log10 FDR
Log2 Fold Change
Tat-4OI vs Tat
Tat-Coc-4OI vs Tat-Coc
4OI vs Control
Anti-Inflammatory Pathways
Antioxidant Activity
Glutathione Process
Nrf2 Target Genes
Pro-Inflammatory Pathways
Adaptive Immune Response
Complement Binding
Cytokine Activity
Non-specified
I
J
K
L
M
Control
Coc
4OI
Tat
Tat-4OI
Tat-Coc
Tat-Coc-4OI
Pde8b
Pde9a
Pde4b
Pde5a
P2rx6
P2rx1
P2rx4
P2ry2
P2ry6
Vasp
Itgal
Rac2
Rnd1
Sdc4
Tgm2
Il18
Il21r
Il1a
Il1b
Il1rn
Il17ra
Il4r
Il13ra1
Il1r1
Il17rb
Il7
Tnfsf10
Tnfrsf11b
Tnfrsf1b
Tnfaip8
Tnfrsf14
Tnfaip2
Tnfaip3
Tnfrsf1a
Tnfaip6
Tnfsf9
1.5
1
0.5
0
-0.5
-1
-1.5

◂**Fig. 4** Genome-wide effects of 4OI on primary neuronal cultures treated with Tat and/or cocaine. RNA-seq transcriptomics of primary cortical cultures treated with Tat (6 ng/mL) and/or cocaine (25 μM) with/without 4OI (250 μM). Volcano plot comparing differential gene expression levels of **a** Tat treated samples vs Control, **b** Tat-Cocaine treated samples vs Control, **c** and cocaine treated samples vs Control. Volcano plot comparing the differential gene expression between **d** 4OI vs Control **e** Tat-4OI vs Tat, and **f** Tat-Cocaine-4OI vs Tat-Cocaine conditions. Scatter plot illustrating the effect of 4OI on transcriptomic fold changes of select differentially expressed genes (FDR < 0.05), and how they correlate between Tat-4OI vs Tat against **g** 4OI vs Control and **h** Tat-Cocaine-4OI vs Tat-Cocaine conditions. The colors correspond with the listed gene set pathway, with green representing select anti-inflammatory and magenta representing select pro-inflammatory pathways. Heatmap showing gene expression levels for **i** phosphodiesterase-associated genes, **j** purinergic receptor-associated genes, **k** phagocytic cytoskeleton-associated genes, **l** interleukin superfamily genes, and **m** tumor necrosis factor family genes

Discussion

Previously, we developed and applied a literature mining and transcriptomics-based approach to uncover new compounds that can inhibit neurotoxic outcomes linked to both HIV and drugs of abuse, with the ultimate goal of identifying potential treatments for HAND with concurrent substance use disorders (Aksenova et al. 2019; Sybrandt et al. 2017, 2020). The analysis of transcriptomes involved a well-established model that simulates HAND with comorbid cocaine use disorder (CUD), utilizing primary cortical cultures treated with Tat and cocaine (Aksenov et al. 2006; Aksenova et al. 2019; Bertrand et al. 2015; Midde et al. 2013; Nath et al. 2002; Turchan et al. 2001). This analysis revealed a significant upregulation in the expression of Acod1 (aconitate decarboxylase 1) mRNA upon exposure to both Tat and Tat-Cocaine treatment.

The ACOD1 protein catalyzes the conversion of the tricarboxylic acid cycle intermediate cis-aconitate into itaconate, an immunometabolite produced during inflammatory responses. Itaconate exhibits potent anti-inflammatory activity (O'Neill and Artyomov 2019) and notably triggers the activation of the anti-inflammatory transcription factor Nrf2 via cysteine thiol alkylation of Keap1, inhibiting Keap1-mediated degradation of Nrf2 (Mills et al. 2018). Further, itaconate establishes tolerance in macrophages exposed to LPS-induced inflammation, hindering late NLRP3 inflammasome activation, IL-1β release, and pyroptosis by dicarboxypropylation of GSDMD (Gasdermin D) (Bambouskova et al. 2021), the main regulator of NLRP3-dependent pyroptosis (Shi et al. 2015), as well as suppresses IL-1α and IL-1β secretion (He et al. 2015; Tsuchiya et al. 2021). Consequently, itaconate orchestrates the regulation of tolerance and the overall level of inflammatory response in macrophages.

Given itaconate's widely recognized anti-inflammatory properties and its potential as a therapeutic candidate for various conditions like sepsis, pulmonary inflammation, lupus, and multiple sclerosis (Lin et al. 2021), we conducted experiments to investigate the possibility of inducing an itaconate-mediated anti-inflammatory response in our HAND-CUD model by utilizing a cell-penetrable analog of this metabolite. Indeed, the ester-modified 4OI showed a potent anti-inflammatory activity in this model. Note that 4OI is also capable of penetrating the blood–brain barrier.

Using primary cortical cultures, we observed a significant increase in cell death when Tat and cocaine were administered together, indicating the synergistic and detrimental neurotoxic effects of this combination (Fig. 1C-B, Supplemental Fig. 1). However, 4OI treatment robustly rescued cellular survival. Excitingly, 4OI was shown to inhibit neuronal apoptosis triggered by Tat and cocaine treatment in a dose-dependent manner (Fig. 1C-D). This suggests that 4OI has the ability to mitigate the toxic effects induced by Tat and cocaine and consequently could be a potential brain-penetrant neuroprotective agent.

Given the specific association of Acod1 expression with inflammation-induced microglia (Sousa et al. 2018), we subsequently proceeded to determine the effects of 4OI on microglia. Pathological stimuli are known to trigger changes in microglial morphology, which is closely linked to their functional states. These states can be categorized as "ramified resting" and "activated ameboid" (Karperien et al. 2013), with various intermediate forms in between. When exposed to detrimental environmental conditions, initially ramified and quiescent microglial cells transition into an intermediate form, characterized by reduced arborization and enlarged soma. Eventually these cells adopt an amoeboid morphology, involving process retraction and increased cell body sizes, which indicates enhanced motility and activity (Davis et al. 2017; Ekdahl 2012; Walker et al. 2013).

Tat and cocaine treatment revealed a concentration-dependent impact on microglia morphology, including an increase in microglial cell number, a shortening of the microglia processes, and an increase in microglia size, with the exception of the highest tested combination concentration, at which survival was substantially compromised (Fig. 3A-C). The percentage of Iba1-positive cells within the culture decreased, and microglia transitioned into a dystrophic state, characterized by spheroidal swelling and stripped ramifications and processes (Holloway et al. 2019) (Fig. 3A-C). Although it appeared by morphology that 4OI and Tat, Tat/cocaine treatments all shift microglial morphology to ameboid, the RNA-seq results suggest that 4OI treatment results in a non-inflammatory ameboid microglia, which have been reported in normal neonatal and adult brains (Orlowski et al. 2003; Silva et al. 2021).

In line with previous observations, 4OI treatment led to a significant activation of Nrf2-regulated antioxidant genes (Peace and O'Neill 2022; Saha et al. 2020; Simpson and

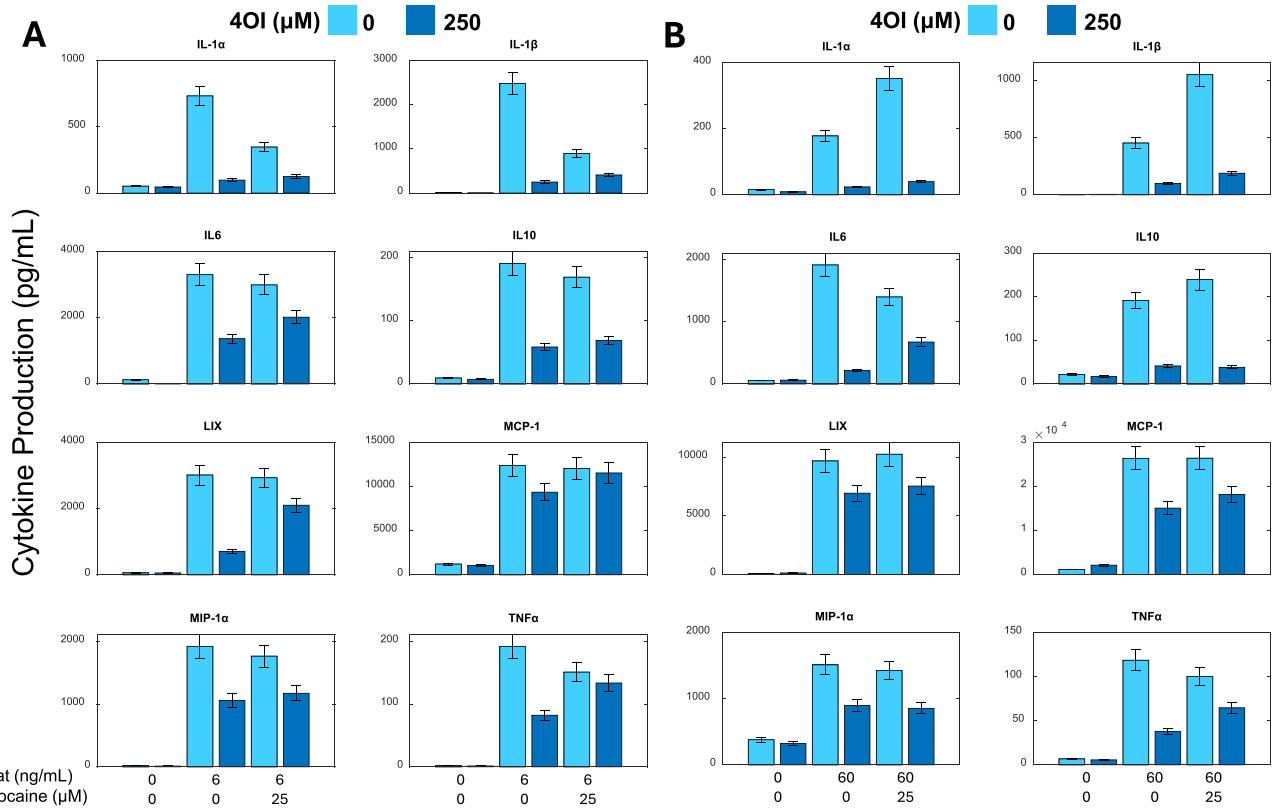

Fig. 5 Effects of 4OI on cytokine secretion profile in primary neuronal cultures treated with Tat and/or cocaine. Bar graphs showing the levels of cytokine secretion followed by Tat 6 ng/mL (**A**) or 60 ng/ml (**B**) and Tat-Cocaine (25 μM), with or without 4OI (250 μM). The cytokine levels were determined by the 27-plex chemokine/cytokine array thrice from each sample of collected cell culture. Bars represent chemokine/cytokine concentrations in the medium (pg/ml) ± SD

Oliver 2020) in both untreated primary cortical cultures and those exposed to Tat and cocaine (Fig. 4). Furthermore, 4OI treatment suppressed the activation of pro-inflammatory pathways specific to myeloid cells, including ones like the adaptive immune response and complement binding. These pathways, typically set in motion by Tat and Tat-Cocaine, are known to be activated by HIV proteins through Toll-like receptor dependent pathways (Donninelli et al. 2016). In agreement with RNA-seq data, the secretion of pro-inflammatory cytokines such as IL-1α, IL-1β, IL6, TNF-α and MIP-1α were activated by Tat and Tat-Cocaine and suppressed by 4OI.

Interestingly, the effects of 4OI on the number of microglial cells were context dependent. While 4OI treatment increased the number of cells in control and Tat-treated cultures, 4OI conversely decreased the amount of microglial cells in Tat-Cocaine exposed cultures (Fig. 3). These results could be attributed to the previously-documented cell- and condition-specific effects associated with Nrf2 activation on cellular proliferation, which can yield either pro- or anti-proliferative effects (Murakami and Motohashi 2015). The cell and condition specific contexts that contribute to pro- or anti-proliferative effects in our model system require further investigation in future studies.

Moreover, 4OI treatment countered the Tat and Tat-Cocaine dependent upregulation of Phosphodiesterases (Pde4b and Pde5a) and Purinergic receptors (P2ry2, P2ry6 and P2rx4). Phosphodiesterases, especially those of Pde4 and Pde5 families, are well-known regulators of microglia activation and serve as targets for the development of small molecules to manage neuroinflammation and treat neurodegenerative diseases, alongside other neuroinflammation-related pathologies (Pearse and Hughes 2016; Sanders 2020). The microglial purinergic receptors are activated by nucleoside di- and triphosphates released by neurons and glial cells in response to both normal brain activity and as a consequences of pathological events (Calovi et al. 2019). Specifically, receptors like P2ry2 and P2ry6, located on the surface of inflammatory microglia, play a role in the induction of phagocytosis and in the removal of stressed neurons (Hide et al. 2023; Puigdellivol et al. 2021). The expression of P2Y receptors is regulated in concert with the genes governing phagocytosis, such as VASP (Montaño-Rendón et al. 2022a), Rac2 (Flannagan et al. 2014) and TGM2 (Rébé et al. 2009).

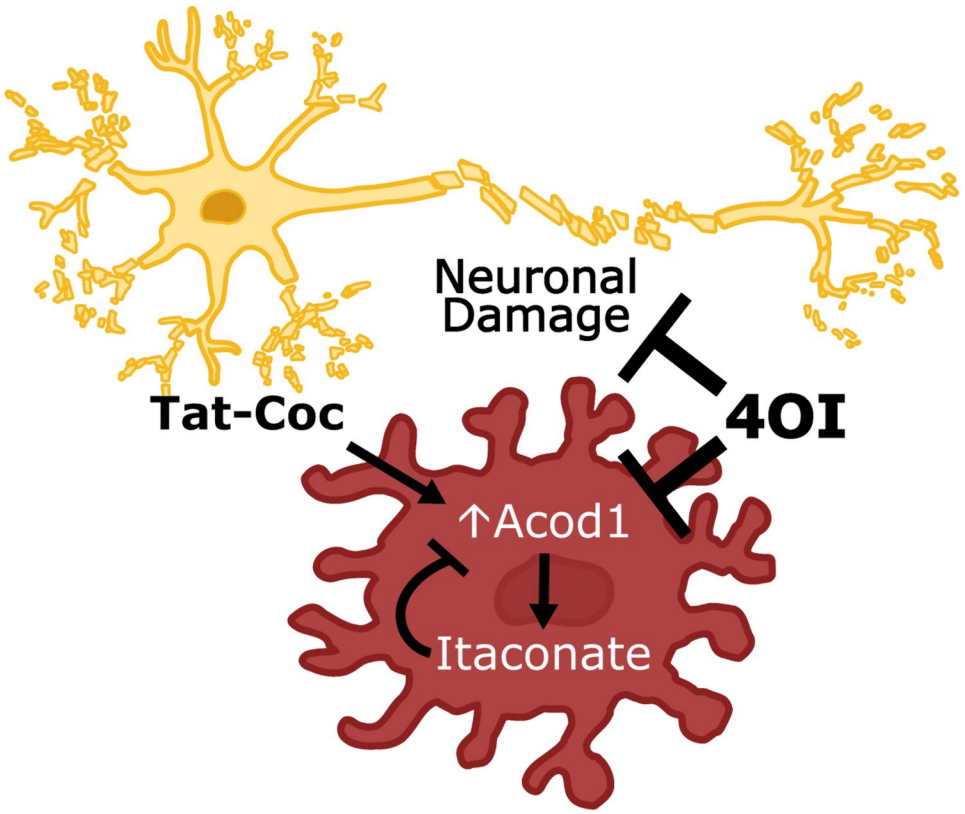

Fig. 6 Possible model of 4OI-mediated neuroprotection. The observed neuronal damage and Acod1 overexpression resulting from Tat and cocaine treatment are significantly attenuated upon 4OI administration. This potential neuroprotection might stem from 4OI's negative feedback inhibition of Acod1

Strikingly one of the most downregulated genes in Tat and Tat-Cocaine treated cultures by 4OI was Acod1. This result points to a potential autoregulatory mechanism of Acod1 expression by its product itaconate that balances activation of itaconate-dependent anti-inflammatory signals in microglial cells (Fig. 6). However, it is also possible that the effects of 4OI could differ from those of endogenous itaconate (Swain et al. 2020). Thus, additional studies are needed to substantiate the presence of such an autoregulatory loop.

Collectively, these findings represent the first exploration of the role of cell-penetrable itaconate esters in microglia activation within the context of HAND-CUD models. Although the precise mechanism of itaconate-dependent microglia activation and regulation requires further studies, the application of the cell- and brain-penetrable form of itaconate, 4OI, holds promise as a potential therapeutic approach for HAND. Furthermore, investigations are warranted to elucidate the underlying mechanisms and evaluate the translational potential of 4OI in treating neuroinflammatory disorders and other neurodegenerative diseases.

Supplementary Information The online version contains supplementary material available at https://doi.org/10.1007/s13365-024-01216-9.

Acknowledgements We thank COBRE Center for Targeted Therapeutics, Microscopy and Flow Cytometry Core for image analysis and Functional Genomics Core for transcriptomics analysis. The COBRE CTT cores are supported by NIH NIGMS P20GM109091. The work was supported by awards from NIH NIDA R21DA058586 (MS, RB, NF), R01DA054992 (MS, MDW).

Author contributions BCC, MA, MS, NF and MDW initiated the study, BCC, VS, MA, DO, DA, EK, HJ, MS, MDW, NF, RB, EB designed and performed experiments, CCB, VS, EB, AS, NF, RB, MS and MDW analyzed the data and provided critical suggestions, BCC, AS, HJ and VS performed image analysis, bioinformatics and statistical analysis, BCC, NF, RB, MDW and MS wrote the manuscript.

Funding Open access funding provided by the Carolinas Consortium. National Institute on Drug Abuse,DA058586,MICHAEL S SHTUTMAN,DA058586,Norma Frizzell,DA058586,Rosemarie Booze,R01DA054992,MICHAEL S SHTUTMAN,R01DA054992,Michael D. Wyatt,National Institute of General Medical Sciences,P20GM109091,MICHAEL S SHTUTMAN

Data availability The RNA-seq data reported in this article has been deposited in NCBI's Gene Expression Omnibus (GEO) and are accessible through GEO Series accession number GSE269380.

Declarations

Conflict of interest None of the authors have any conflict of interest.

Open Access This article is licensed under a Creative Commons Attribution 4.0 International License, which permits use, sharing, adaptation, distribution and reproduction in any medium or format, as long as you give appropriate credit to the original author(s) and the source, provide a link to the Creative Commons licence, and indicate if changes were made. The images or other third party material in this article are included in the article's Creative Commons licence, unless indicated otherwise in a credit line to the material. If material is not included in

the article's Creative Commons licence and your intended use is not permitted by statutory regulation or exceeds the permitted use, you will need to obtain permission directly from the copyright holder. To view a copy of this licence, visit http://creativecommons.org/licenses/by/4.0/.

References

Aksenov MY, Aksenova MV, Nath A, Ray PD, Mactutus CF, Booze RM (2006) Cocaine-mediated enhancement of Tat toxicity in rat hippocampal cell cultures: the role of oxidative stress and D1 dopamine receptor. Neurotoxicology 27:217–228

Aksenova MV, Aksenov MY, Adams SM, Mactutus CF, Booze RM (2009) Neuronal survival and resistance to HIV-1 Tat toxicity in the primary culture of rat fetal neurons. Exp Neurol 215:253–263

Aksenova M, Sybrandt J, Cui B, Sikirzhytski V, Ji H, Odhiambo D, Lucius MD, Turner JR, Broude E, Pena E, Lizarraga S, Zhu J, Safro I, Wyatt MD, Shtutman M (2019) Inhibition of the dead box RNA helicase 3 prevents HIV-1 Tat and cocaine-induced neurotoxicity by targeting microglia activation. J Neuroimmune Pharmacol 15(2):209–223

Anwar S, Pons V (2020) Rivest S (2020) Microglia purinoceptor P2Y6: an emerging therapeutic target in CNS diseases. Cells 9(7):1595

Atluri VS (2016) Editorial: HIV and Illicit Drugs of Abuse. Front Microbiol 7:221

Avants SK, Margolin A, McMahon TJ, Kosten TR (1997) Association between self-report of cognitive impairment, HIV status, and cocaine use in a sample of cocaine-dependent methadone-maintained patients. Addict Behav 22:599–611

Bambouskova M, Potuckova L, Paulenda T, Kerndl M, Mogilenko DA, Lizotte K, Swain A, Hayes S, Sheldon RD, Kim H, Kapadnis U, Ellis AE, Isaguirre C, Burdess S, Laha A, Amarasinghe GK, Chubukov V, Roddy TP, Diamond MS, Jones RG, Simons DM, Artyomov MN (2021) Itaconate confers tolerance to late NLRP3 inflammasome activation. Cell Rep 34:108756

Ben Haij N, Planes R, Leghmari K, Serrero M, Delobel P, Izopet J, BenMohamed L, Bahraoui E (2015) HIV-1 Tat protein induces production of pro-inflammatory cytokines by human dendritic cells and monocytes/macrophages through engagement of TLR4-MD2-CD14 complex and activation of NF-kappaB pathway. PLoS ONE 10:e0129425

Bertrand SJ, Hu C, Aksenova MV, Mactutus CF, Booze RM (2015) HIV-1 Tat and cocaine mediated synaptopathy in cortical and midbrain neurons is prevented by the isoflavone Equol. Front Microbiol 6:894

Beyrer C, Wirtz AL, Baral S, Peryskina A, Sifakis F (2010) Epidemiologic links between drug use and HIV epidemics: an international perspective. J Acquir Immune Defic Syndr 55(Suppl 1):S10–S16

Biber K, Bhattacharya A, Campbell BM, Piro JR, Rohe M, Staal RGW, Talanian RV, Möller T (2019) Microglial drug targets in AD: opportunities and challenges in drug discovery and development. Front Pharmacol 10:840

Calovi S, Mut-Arbona P, Sperlagh B (2019) Microglia and the purinergic signaling system. Neuroscience 405:137–147

Catale C, Bussone S, Lo Iacono L, Carola V (2019) Microglial alterations induced by psychoactive drugs: A possible mechanism in substance use disorder? Semin Cell Dev Biol 94:164–175

Daniels BP, Kofman SB, Smith JR, Norris GT, Snyder AG, Kolb JP, Gao X, Locasale JW, Martinez J, Gale M Jr, Loo YM, Oberst A (2019) The Nucleotide Sensor ZBP1 and Kinase RIPK3 induce the Enzyme IRG1 to promote an antiviral metabolic state in neurons. Immunity 50(64–76):e4

Davis BM, Salinas-Navarro M, Cordeiro MF, Moons L, De Groef L (2017) Characterizing microglia activation: a spatial statistics approach to maximize information extraction. Sci Rep 7:1576

Dobin A, Davis CA, Schlesinger F, Drenkow J, Zaleski C, Jha S, Batut P, Chaisson M, Gingeras TR (2013) STAR: ultrafast universal RNA-seq aligner. Bioinformatics 29:15–21

Donninelli G, Gessani S, Del Cornò M (2016) Interplay between HIV-1 and Toll-like receptors in human myeloid cells: friend or foe in HIV-1 pathogenesis? J Leukoc Biol 99:97–105

Ekdahl CT (2012) Microglial activation – tuning and pruning adult neurogenesis. Front Pharmacol 2012(3):41

Flannagan RS, Canton J, Furuya W, Glogauer M, Grinstein S (2014) The phosphatidylserine receptor TIM4 utilizes integrins as coreceptors to effect phagocytosis. Mol Biol Cell 25:1511–1522

Gannon P, Khan MZ, Kolson DL (2011) Current understanding of HIV-associated neurocognitive disorders pathogenesis. Curr Opin Neurol 24:275–283

Hanisch UK (2002) Microglia as a source and target of cytokines. Glia 40:140–155

Harper J, Ribeiro SP, Chan CN, Aid M, Deleage C, Micci L, Pino M, Cervasi B, Raghunathan G, Rimmer E, Ayanoglu G, Wu G, Shenvi N, Barnard RJ, Del Prete GQ, Busman-Sahay K, Silvestri G, Kulpa DA, Bosinger SE, Easley KA, Howell BJ, Gorman D, Hazuda DJ, Estes JD, Sekaly RP, Paiardini M (2022) Interleukin-10 contributes to reservoir establishment and persistence in SIV-infected macaques treated with antiretroviral therapy. J Clin Invest 132(8):e155251

He WT, Wan H, Hu L, Chen P, Wang X, Huang Z, Yang ZH, Zhong CQ, Han J (2015) Gasdermin D is an executor of pyroptosis and required for interleukin-1β secretion. Cell Res 25:1285–1298

Hide I, Shiraki H, Masuda A, Maeda T, Kumagai M, Kunishige N, Yanase Y, Harada K, Tanaka S, Sakai N (2023) P2Y2 receptor mediates dying cell removal via inflammatory activated microglia. J Pharmacol Sci 153:55–67

Holloway OG, Canty AJ, King AE, Ziebell JM (2019) Rod microglia and their role in neurological diseases. Semin Cell Dev Biol 94:96–103

Karn J, Stoltzfus CM (2012) Transcriptional and posttranscriptional regulation of HIV-1 gene expression. Cold Spring Harb Perspect Med 2:a006916

Karperien A, Ahammer H, Jelinek HF (2013) Quantitating the subtleties of microglial morphology with fractal analysis. Front Cell Neurosci 7:3

Lampropoulou V, Sergushichev A, Bambouskova M, Nair S, Vincent EE, Loginicheva E, Cervantes-Barragan L, Ma X, Huang SC, Griss T, Weinheimer CJ, Khader S, Randolph GJ, Pearce EJ, Jones RG, Diwan A, Diamond MS, Artyomov MN (2016) Itaconate links inhibition of succinate dehydrogenase with macrophage metabolic remodeling and regulation of inflammation. Cell Metab 24:158–166

Liao Y, Smyth GK, Shi W (2014) featureCounts: an efficient general purpose program for assigning sequence reads to genomic features. Bioinformatics 30:923–930

Liao K, Guo M, Niu F, Yang L, Callen SE, Buch S (2016) Cocaine-mediated induction of microglial activation involves the ER stress-TLR2 axis. J Neuroinflammation 13:33

Lin J, Ren J, Gao DS, Dai Y, Yu L (2021) The emerging application of itaconate: promising molecular targets and therapeutic opportunities. Front Chem 9:669308

Liu C-Y, Wang X, Liu C, Zhang H-L (2019) Pharmacological targeting of microglial activation: new therapeutic approach. Front Cell Neurosci 13:514

Marcus JL, Leyden WA, Alexeeff SE, Anderson AN, Hechter RC, Hu H, Lam JO, Towner WJ, Yuan Q, Horberg MA, Silverberg MJ (2020) Comparison of overall and comorbidity-free life expectancy between insured adults with and without HIV infection, 2000–2016. JAMA Netw Open 3:e207954

McCarthy DJ, Chen Y, Smyth GK (2012) Differential expression analysis of multifactor RNA-Seq experiments with respect to biological variation. Nucleic Acids Res 40:4288–4297

Michelucci A, Cordes T, Ghelfi J, Pailot A, Reiling N, Goldmann O, Binz T, Wegner A, Tallam A, Rausell A, Buttini M, Linster CL, Medina E, Balling R, Hiller K (2013) Immune-responsive gene 1 protein links metabolism to immunity by catalyzing itaconic acid production. Proc Natl Acad Sci U S A 110:7820–7825

Midde NM, Huang X, Gomez AM, Booze RM, Zhan CG, Zhu J (2013) Mutation of tyrosine 470 of human dopamine transporter is critical for HIV-1 Tat-induced inhibition of dopamine transport and transporter conformational transitions. J Neuroimmune Pharmacol 8:975–987

Mills EL, Ryan DG, Prag HA, Dikovskaya D, Menon D, Zaslona Z, Jedrychowski MP, Costa ASH, Higgins M, Hams E, Szpyt J, Runtsch MC, King MS, McGouran JF, Fischer R, Kessler BM, McGettrick AF, Hughes MM, Carroll RG, Booty LM, Knatko EV, Meakin PJ, Ashford MLJ, Modis LK, Brunori G, Sévin DC, Fallon PG, Caldwell ST, Kunji ERS, Chouchani ET, Frezza C, Dinkova-Kostova AT, Hartley RC, Murphy MP, O'Neill LA (2018) Itaconate is an anti-inflammatory metabolite that activates Nrf2 via alkylation of KEAP1. Nature 556:113–117

Montaño-Rendón F, Walpole GFW, Krause M, Hammond GRV, Grinstein S, Fairn GD (2022a) PtdIns(3,4)P2, Lamellipodin, and VASP coordinate actin dynamics during phagocytosis in macrophages. J Cell Biol 221(11):e202207042

Montaño-Rendón F, Walpole GFW, Krause M, Hammond GRV, Grinstein S, Fairn GD (2022b) PtdIns(3,4)P2, Lamellipodin, and VASP coordinate actin dynamics during phagocytosis in macrophages. J Cell Biol 221

Murakami S, Motohashi H (2015) Roles of Nrf2 in cell proliferation and differentiation. Free Radic Biol Med 88:168–178

Nath A (2002) Human immunodeficiency virus (HIV) proteins in neuropathogenesis of HIV dementia. J Infect Dis 186(Suppl 2):S193–S198

Nath A, Hauser KF, Wojna V, Booze RM, Maragos W, Prendergast M, Cass W, Turchan JT (2002) Molecular basis for interactions of HIV and drugs of abuse. J Acquir Immune Defic Syndr 31(Suppl 2):S62–S69

Ni L, Xiao J, Zhang D, Shao Z, Huang C, Wang S, Wu Y, Tian N, Sun L, Wu A, Zhou Y, Wang X, Zhang X (2022) Immune-responsive gene 1/itaconate activates nuclear factor erythroid 2-related factor 2 in microglia to protect against spinal cord injury in mice. Cell Death Dis 13:140

NIDA (2018) Monitoring the Future 2018 Survey Results. National Survey Results on Drug Use, 1975-2023

Olagnier D, Farahani E, Thyrsted J, Blay-Cadanet J, Herengt A, Idorn M, Hait A, Hernaez B, Knudsen A, Iversen MB, Schilling M, Jorgensen SE, Thomsen M, Reinert LS, Lappe M, Hoang HD, Gilchrist VH, Hansen AL, Ottosen R, Nielsen CG, Moller C, van der Horst D, Peri S, Balachandran S, Huang J, Jakobsen M, Svenningsen EB, Poulsen TB, Bartsch L, Thielke AL, Luo Y, Alain T, Rehwinkel J, Alcami A, Hiscott J, Mogensen TH, Paludan SR, Holm CK (2020a) Author Correction: SARS-CoV2-mediated suppression of NRF2-signaling reveals potent antiviral and anti-inflammatory activity of 4-octyl-itaconate and dimethyl fumarate. Nat Commun 11:5419

Olagnier D, Farahani E, Thyrsted J, Blay-Cadanet J, Herengt A, Idorn M, Hait A, Hernaez B, Knudsen A, Iversen MB, Schilling M, Jorgensen SE, Thomsen M, Reinert LS, Lappe M, Hoang HD, Gilchrist VH, Hansen AL, Ottosen R, Nielsen CG, Moller C, van der Horst D, Peri S, Balachandran S, Huang J, Jakobsen M, Svenningsen EB, Poulsen TB, Bartsch L, Thielke AL, Luo Y, Alain T, Rehwinkel J, Alcami A, Hiscott J, Mogensen TH, Paludan SR, Holm CK (2020b) SARS-CoV2-mediated suppression of NRF2-signaling reveals potent antiviral and anti-inflammatory activity of 4-octyl-itaconate and dimethyl fumarate. Nat Commun 11:4938

O'Neill LAJ, Artyomov MN (2019) Itaconate: the poster child of metabolic reprogramming in macrophage function. Nat Rev Immunol 19:273–281

Orlowski D, Soltys Z, Janeczko K (2003) Morphological development of microglia in the postnatal rat brain. A quantitative study. Int J Dev Neurosci 21:445–450

Osborne O, Peyravian N, Nair M, Daunert S, Toborek M (2020) The paradox of HIV blood-brain barrier penetrance and antiretroviral drug delivery deficiencies. Trends Neurosci 43:695–708

Peace CG, O'Neill LA (2022) The role of itaconate in host defense and inflammation. J Clin Invest 132(2):e148548

Pearse DD, Hughes ZA (2016) PDE4B as a microglia target to reduce neuroinflammation. Glia 64:1698–1709

Puigdellivol M, Milde S, Vilalta A, Cockram TOJ, Allendorf DH, Lee JY, Dundee JM, Pampuscenko K, Borutaite V, Nuthall HN, Brelstaff JH, Spillantini MG, Brown GC (2021) The microglial P2Y(6) receptor mediates neuronal loss and memory deficits in neurodegeneration. Cell Rep 37:110148

Rébé C, Raveneau M, Chevriaux A, Lakomy D, Sberna AL, Costa A, Bessède G, Athias A, Steinmetz E, Lobaccaro JM, Alves G, Menicacci A, Vachenc S, Solary E, Gambert P, Masson D (2009) Induction of transglutaminase 2 by a liver X receptor/retinoic acid receptor alpha pathway increases the clearance of apoptotic cells by human macrophages. Circ Res 105:393–401

Robinson MD, McCarthy DJ, Smyth GK (2010) edgeR: a Bioconductor package for differential expression analysis of digital gene expression data. Bioinformatics 26:139–140

Saha S, Buttari B, Panieri E, Profumo E, Saso L (2020) An overview of Nrf2 signaling pathway and its role in inflammation. Molecules 25(22):5474

Samikkannu T, Atluri VS, Nair MP (2016) HIV and cocaine impact glial metabolism: energy sensor AMP-activated protein kinase role in mitochondrial biogenesis and epigenetic remodeling. Sci Rep 6:31784

Sanders O (2020) Sildenafil for the treatment of alzheimer's disease: a systematic review. J Alzheimers Dis Rep 4:91–106

Saylor D, Dickens AM, Sacktor N, Haughey N, Slusher B, Pletnikov M, Mankowski JL, Brown A, Volsky DJ, McArthur JC (2016) HIV-associated neurocognitive disorder–pathogenesis and prospects for treatment. Nat Rev Neurol 12:234–248

Shi J, Zhao Y, Wang K, Shi X, Wang Y, Huang H, Zhuang Y, Cai T, Wang F, Shao F (2015) Cleavage of GSDMD by inflammatory caspases determines pyroptotic cell death. Nature 526:660–665

Silva NJ, Dorman LC, Vainchtein ID, Horneck NC, Molofsky AV (2021) In situ and transcriptomic identification of microglia in synapse-rich regions of the developing zebrafish brain. Nat Commun 12:5916

Simpson DSA, Oliver PL (2020) ROS generation in microglia: understanding oxidative stress and inflammation in neurodegenerative disease. Antioxidants (Basel) 9(8):743

Sohail A, Iqbal AA, Sahini N, Chen F, Tantawy M, Waqas SFH, Winterhoff M, Ebensen T, Schultz K, Geffers R, Schughart K, Preusse M, Shehata M, Bahre H, Pils MC, Guzman CA, Mostafa A, Pleschka S, Falk C, Michelucci A, Pessler F (2022a) Correction: Itaconate and derivatives reduce interferon responses and inflammation in influenza A virus infection. PLoS Pathog 18:e1011002

Sohail A, Iqbal AA, Sahini N, Chen F, Tantawy M, Waqas SFH, Winterhoff M, Ebensen T, Schultz K, Geffers R, Schughart K, Preusse M, Shehata M, Bahre H, Pils MC, Guzman CA, Mostafa A, Pleschka S, Falk C, Michelucci A, Pessler F (2022b) Itaconate and derivatives reduce interferon responses and inflammation in influenza A virus infection. PLoS Pathog 18:e1010219

Sophocleous RA, Ooi L, Sluyter R (2022) The P2X4 receptor: cellular and molecular characteristics of a promising neuroinflammatory target. Int J Mol Sci 23(10):5739

Sousa C, Golebiewska A, Poovathingal SK, Kaoma T, Pires-Afonso Y, Martina S, Coowar D, Azuaje F, Skupin A, Balling R, Biber K, Niclou SP, Michelucci A (2018) Single-cell transcriptomics reveals distinct inflammation-induced microglia signatures. EMBO Rep 19:e46171

Spiehler VR, Reed D (1985) Brain concentrations of cocaine and benzoylecgonine in fatal cases. J Forensic Sci 30:1003–1011

Sreeram S, Ye F, Garcia-Mesa Y, Nguyen K, El Sayed A, Leskov K, Karn J (2022) The potential role of HIV-1 latency in promoting neuroinflammation and HIV-1-associated neurocognitive disorder. Trends Immunol 43:630–639

Swain A, Bambouskova M, Kim H, Andhey PS, Duncan D, Auclair K, Chubukov V, Simons DM, Roddy TP, Stewart KM, Artyomov MN (2020) Comparative evaluation of itaconate and its derivatives reveals divergent inflammasome and type I interferon regulation in macrophages. Nat Metab 2:594–602

Sybrandt J, Shtutman M, Safro I (2017) MOLIERE: automatic biomedical hypothesis generation system. KDD : Proc Int Conf Knowl Discov Data Mining 2017:1633–1642

Sybrandt J, Tyagin I, Shtutman M, Safro I (2020) AGATHA: Automatic Graph Mining And Transformer Based Hypothesis Generation Approach. Assoc Comput Machinery 2757–2764, arXiv:2002.05635v1

Tsuchiya K, Hosojima S, Hara H, Kushiyama H, Mahib MR, Kinoshita T, Suda T (2021) Gasdermin D mediates the maturation and release of IL-1alpha downstream of inflammasomes. Cell Rep 34:108887

Turchan J, Anderson C, Hauser KF, Sun Q, Zhang J, Liu Y, Wise PM, Kruman I, Maragos W, Mattson MP, Booze R, Nath A (2001) Estrogen protects against the synergistic toxicity by HIV proteins, methamphetamine and cocaine. BMC Neurosci 2:3

Walker FR, Nilsson M, Jones K (2013) Acute and chronic stress-induced disturbances of microglial plasticity, phenotype and function. Curr Drug Targets 14:1262–1276

Wallet C, De Rovere M, Van Assche J, Daouad F, De Wit S, Gautier V, Mallon PWG, Marcello A, Van Lint C, Rohr O, Schwartz C (2019) Microglial Cells: The Main HIV-1 Reservoir in the Brain. Front Cell Infect Microbiol 9:362

Westendorp MO, Frank R, Ochsenbauer C, Stricker K, Dhein J, Walczak H, Debating K-M, Krammer PH (1995) Sensitization of T cells to CD95-mediated apoptosis by HIV-1 Tat and gp120. Nature 375:497–500

Xiao H, Neuveut C, Tiffany HL, Benkirane M, Rich EA, Murphy PM, Jeang KT (2000) Selective CXCR4 antagonism by Tat: implications for in vivo expansion of coreceptor use by HIV-1. Proc Natl Acad Sci U S A 97:11466–11471

Yuan Y, Huang X, Midde NM, Quizon PM, Sun WL, Zhu J, Zhan CG (2015) Molecular mechanism of HIV-1 Tat interacting with human dopamine transporter. ACS Chem Neurosci 6:658–665

Zayyad Z, Spudich S (2015) Neuropathogenesis of HIV: from initial neuroinvasion to HIV-associated neurocognitive disorder (HAND). Curr HIV/AIDS Rep 12:16–24

Zhao X, Zhang F, Kandel SR, Brau F, He JJ (2022) HIV Tat and cocaine interactively alter genome-wide DNA methylation and gene expression and exacerbate learning and memory impairments. Cell Rep 39:110765

Zimmer BA, Dobrin CV, Roberts DC (2011) Brain-cocaine concentrations determine the dose self-administered by rats on a novel behaviorally dependent dosing schedule. Neuropsychopharmacology 36:2741–2749

Publisher's Note Springer Nature remains neutral with regard to jurisdictional claims in published maps and institutional affiliations.